

Acceleration of radiation transitions in a cylindrical cavity: study of the dependence on the position of the radiation dipole using the example of luminol chemiluminescence in cavities of a thin aluminum film

© N.S. Petrov, D.R. Dadadzhanov, T.A. Vartanyan

ITMO University, St. Petersburg, Russia

e-mail: tavartanyan@itmo.ru

Received December 03, 2025

Revised December 03, 2025

Accepted December 08, 2025

This paper presents the results of numerical modeling of acceleration of radiative transitions for a luminol molecule in the dipole approximation while it is located within cylindrical cutouts in a thin perforated aluminum film. The calculations were performed considering various dipole orientations and dipole position within the cavities. It is shown that the metasurface significantly increases the molecule's radiative decay rate, reaching values greater than 45 as the dipole approaches the metal surface. The distribution of radiation acceleration was determined depending on the height above the substrate and the radial position. Spectral analysis revealed a high overlap of the Purcell factor maximum with the luminol chemiluminescence spectrum, confirming the potential of the proposed structure for amplifying chemiluminescent signals in biosensors.

Keywords: radiative transitions, chemiluminescence, plasmon resonance, luminol.

DOI: 10.61011/EOS.2026.02.63470.8841-25

Introduction

It has become common in the modern world to use materials and technologies related to luminescence. Starting from habitual fluorescent lamps and ending with most sophisticated technologies of TV QLED matrix operation, luminescence plays a key role everywhere. All-round application and comprehensive research of luminescent processes make it possible to hope that in the nearest future the luminescent technologies will become even more affordable and reliable, which will enable their introduction into such demanding sphere as biomedicine.

Among biomedical applications of luminescence, methods based on chemiluminescence play a special role [1]. Using chemiluminescence, various diseases may be diagnosed, quality of pharmacological synthesis may be identified and, which is especially important, active forms of oxygen may be found in biosamples [2–4].

The substantial advantage of chemiluminescent methods compared to other optical methods used in biomedicine is the absence of the need for the source of light, since the light arises as a result of the studied chemical reaction as such. This enables equipment simplification and reduction of its dimensions, which could result in reduction of its cost and wider use. Unfortunately, the quantum yield of chemiluminescence in biologically compatible systems is low [5], which makes the task of its increase exceptionally important for the practical applications of chemiluminescence. One of the promising ways to increase the quantum yield of chemiluminescence consists in acceleration of the final radiation transition, which may be achieved through Purcell effect, i.e. at the expense of the placement of

the radiating molecule into the area of the space with the modified density of radiation modes.

The idea to increase the quantum yield of luminescence, including chemiluminescence, at the expense of the acceleration of radiation processes has been developing actively from the beginning of this century. The review of early papers on this subject may be found in [6]. Reinforcement of chemiluminescence near various metal nanostructures with resonances of plasmon type was demonstrated experimentally [7–10]. According to the modeling results [8], acceleration of radiation transitions may be significant, however, its value depends strongly on the molecule position relative to the nanoparticle. In connection with it the Purcell factor calculations are of interest regarding the structures, where one can expect a more even distribution of the radiation transition acceleration factor in the space that may be occupied with radiating molecules. As it is shown in [11], the promising structure for acceleration of the radiation transitions of the most popular chemiluminescent molecule — luminol molecule — is a thin aluminum film with periodically arranged holes.

This paper is dedicated to the calculation of the radiation intensity in the dipole emitter modeling radiation transitions in the luminol molecule, depending on its orientation and the position inside the cylindrical cavity in the thin aluminum film. Thickness of the film and diameter of the openings located in the nodes of the square lattice are selected so that the maximum acceleration of radiation transitions is provided in the luminol chemiluminescence maximum.

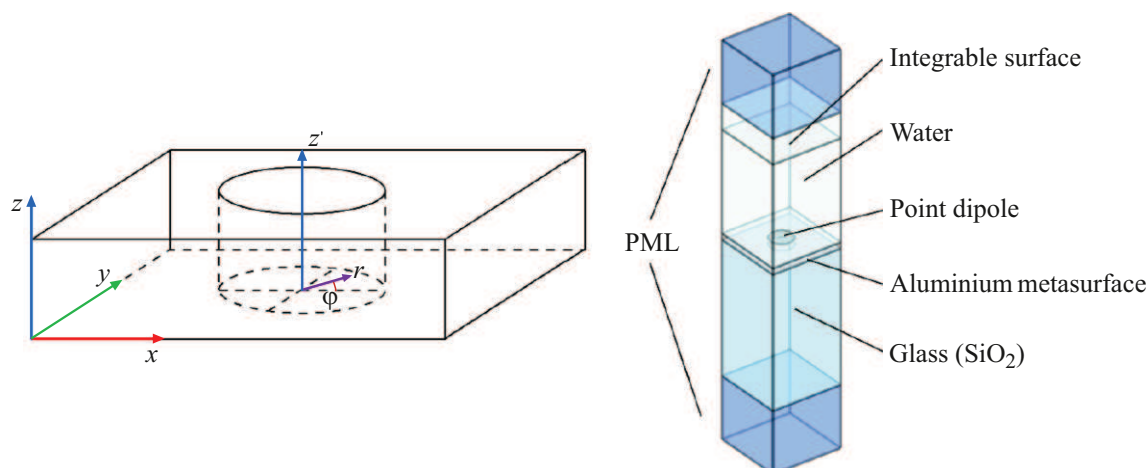


Figure 1. Diagram of lattice cell used in modeling. The pores were assumed to be fully saturated with the target medium, with its refractive index set equivalent to that of water.

Materials and methods

Acceleration of radiation transitions is studied at wavelength of 430 nm — in the maximum of luminol chemiluminescence band. It is assumed that the luminol molecules with equal probability take various orientations and different positions in the cylindrical cavities of the aluminum film with thickness of 20 nm. Radii of cavities are 36 nm, and their centers are located in the nodes of the square lattice with the period of 230 nm. The aluminum film was located on the substrate from fused silica with refractive index of 1.46. The refractive index of the aqueous medium, which filled the cavities and all the half-space above the film was accepted as equal to 1.33. The optical properties of aluminum were taken from [12]. Selection of the model's geometric parameters depends on previously obtained results [11], which mean that such structure may accelerate the radiation decay of luminol molecules and result in increased quantum yield of luminescence.

The diagram of the used model is shown in Fig. 1. Optical characteristics of the considered metal surface were analyzed in COMSOL Multiphysics software environment with application of the finite element method. The facets of the lattice cell took into account the Floquet's periodicity conditions. Purcell factor F_P was adopted as equal to the ratio of radiation intensity into the upper half-plane of the dipole with certain amplitude placed into the cavity, P_{Al} , to the medium radiation intensity of the arbitrarily orienting dipole with the same amplitude in aqueous medium without a perforated metal film, but in presence of the substrate, P_{free} , i.e. $f_P = P_{Al}/P_{free}$.

The calculations were executed for various orientations and positions of the dipole inside the cavity. To describe the position of the dipole, a cylindrical system of coordinates was used, the origin of which matches the center of circumference formed by the cavity on the substrate, and the axis is perpendicular to the substrate. Therefore, the dipole

could be located at different heights from the substrate z' and at different distances from axis r . Dependence of the calculation results on the azimuthal angle φ , which was counted from axis x , is caused by the effect of the neighboring cavities. For each position the radiation intensities were calculated for the dipoles oriented vertically (in parallel to axis z'), P_{all}^v , radially (to axis z'), P_{all}^r , and azimuthally (in parallel to the tangent to the nearest point of the metal surface), P_{all}^t . It was adopted that all orientations of the emitting dipole inside the cavity were equally probable, and they were used to do averaging.

To study variation of Purcell factor in the volume of the cavity, it was calculated at heights z' , equal to 1, 10 and 20 nm, radial distances r from 0 to 25 nm with pitch of 2 nm and azimuthal angles φ from 0° to 45° with a pitch of 5° . The calculations in a larger range of variation φ are not required in virtue of lattice symmetry.

Purcell factors were not calculated and not presented in this paper for the distances from metal surfaces smaller than 1 nm, since in the specified area the interaction of the molecule with the metal surface causes retuning of the energy structure of the molecule, which may not be described within the electrodynamic calculation. This limitation may not substantially affect the results, since the volume excluded from the consideration was smaller than 6% of the entire cavity volume.

Calculation of acceleration of radiation transitions in cavities of perforated aluminum film

As a result of the completed modeling, the dependences were obtained on the average value of Purcell factor on radius r and angle φ at heights $z' = 1, 10$ and 20 nm. Near the substrate at $z' = 1$ nm (Fig. 2) Purcell factor varies from the least value 8.9 on axis of the cavity at $r = 0$

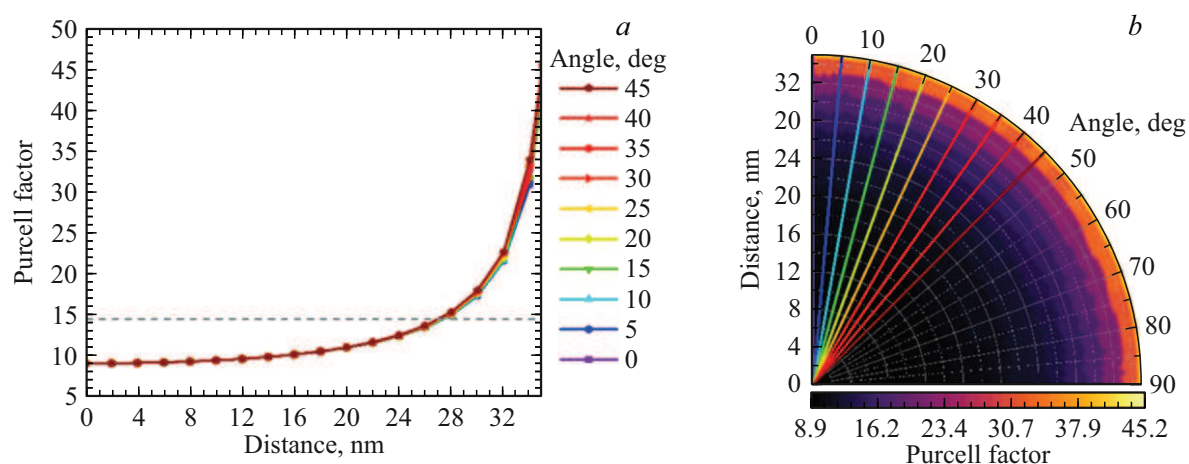


Figure 2. (a) Dependence of Purcell's factor averaged by 3 directions on radius r and on angle φ at height $z' = 1$ nm. The dashed line shows the average value of the Purcell factor at this height equal to 14.4. (b) Color map of cylindrical cut segment at height of $z' = 1$ nm, where color codes the value of Purcell factor that varies from 8.9 to 45.2. Color radial lines indicate directions within 0- 45°, for which the calculations were made.

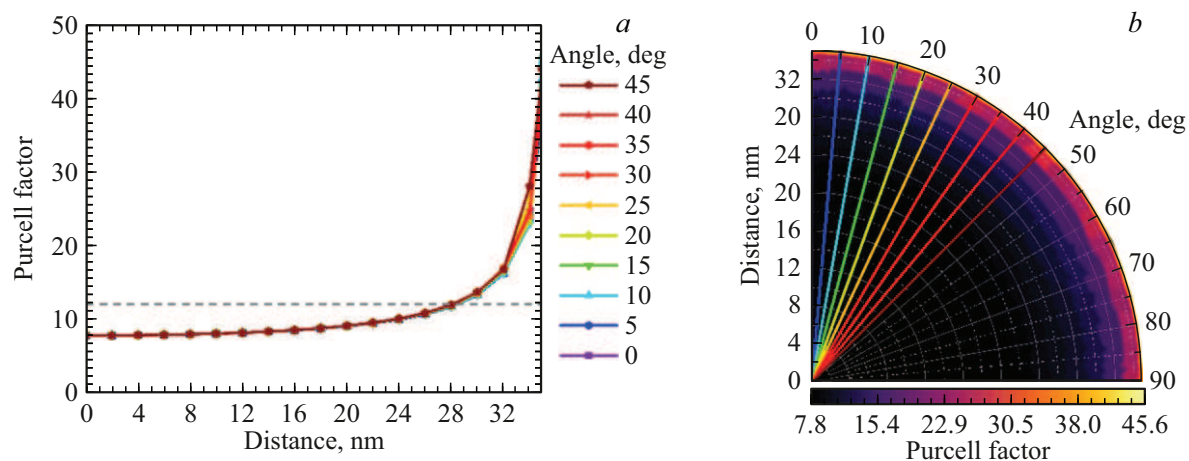


Figure 3. (a) Dependence of Purcell factor averaged by 3 directions on radius r and on angle φ at height $z' = 20$ nm. The dashed line shows average value of Purcell factor at this height, which is 12.1. (b) Color map of cylindrical cut segment at height $z' = 20$ nm, where color codes the value of Purcell factor. Color radial lines indicate directions within 0- 45°, for which the calculations were made.

to the highest one, equal to 45.2 near the metal surface at $r = 35$ nm. Dependence on distance is described well with exponential function. As the dipole approaches the metal surface, Purcell factor increases more than 5 times. At the same time the angular dependence is practically not observed.

Similar results, but with somewhat lower values of Purcell factor were obtained also at the height of the upper edge of the film $z' = 20$ nm (Fig. 3). The least value of Purcell factor equal to 7.8 is in the axis of the cylindrical cavity. As the distance from the axis increases, and the metal surface is approached, Purcell factor increases exponentially, and at the last calculated distance from axis $r = 35$ nm achieves 45.6. The angular dependence is similarly practically absent.

At the intermediate height at $z' = 10$ nm (Fig. 4) somewhat different dependences are observed. The minimum is

similarly found on the axis of the cavity and is equal to 9.3, but instead of monotonic growth as the metal surface is approached at the distance from axis $r = 32$ nm, the highest value of Purcell factor is achieved, equal to 14.3, and with further approach to the metal surface it decreases. Therefore, at this intermediate height, when the metal surface is approached, Purcell factor is not growing as much as at extreme heights $z' = 1$ and 20 nm.

Since the results provided above were based on the calculations for the only wavelength corresponding to the maximum of the luminol chemiluminescence band, the dependence of Purcell factor on wavelength is of interest. In Fig. 5 the spectrum of Purcell factor for the dipole located in the center of the cylindrical cavity ($z' = 10$ nm, $r = 0$), is compared to the normalized spectrum of luminol chemiluminescence. The closeness of the maxima of the given spectra and large area of their overlapping confirms

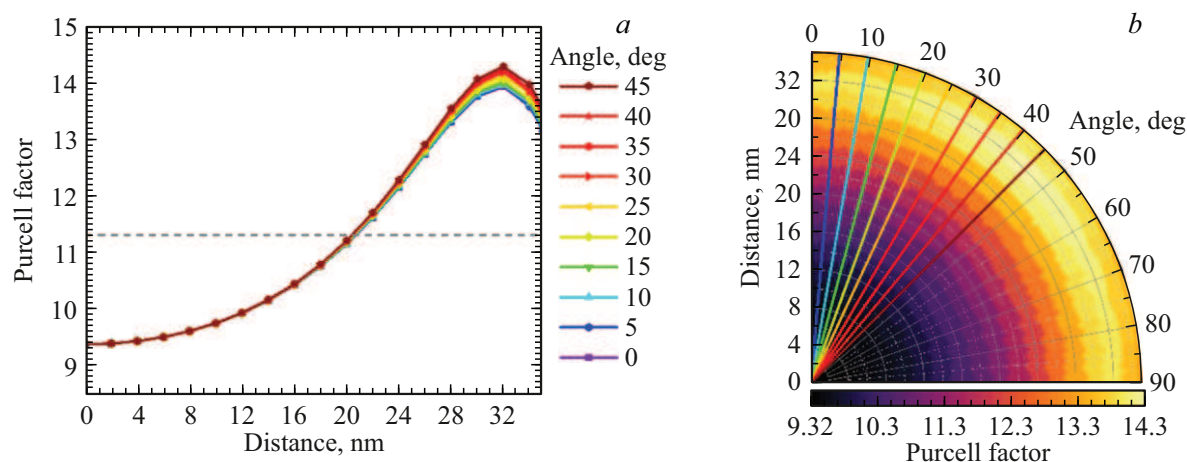


Figure 4. (a) Dependence of Purcell factor averaged by 3 directions on radius r and on angle φ at height $z' = 10$ nm. The dashed line shows average value of Purcell factor at this height, which is 11.3. (b) Color map of cylindrical cut segment at height $z' = 10$ nm, where color codes the value of Purcell factor. Color radial lines indicate directions within 0-45°, for which the calculations were made.

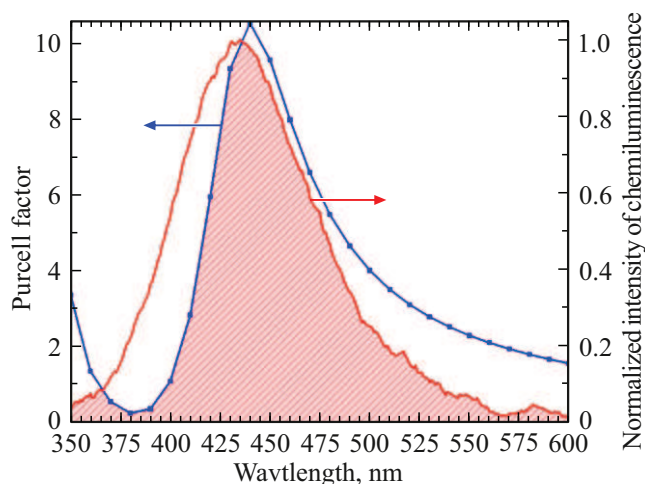


Figure 5. Dependence of Purcell factor averaged in orientations of emitting dipole in the center of the cylindrical cavity (blue curve, left vertical axis), and normalized spectrum of chemiluminescence of luminol (red curve, right vertical axis). In the filled spectral region the substantial part of the chemiluminescent radiation of luminol experiences the acceleration of radiation transitions close to the maximum.

the fitness of the modeled structure to reinforce the luminol chemiluminescence.

Conclusions

The produced results of modeling show that the speed of radiation transitions of luminol molecules placed into cylindrical cavities in the aluminum film increases substantially. Purcell factor averaged in orientations of the emitting dipole increases in all cases as the dipole approaches the metal surface and reaches values above 45. It was established that at heights 1 and 20 nm, i.e. near the substrate and at the

boundary of the metal film, where the metal ribs are located, exponential growth of Purcell factor was observed upon approaching the metal surface, whereas at height of 10 nm, where there are no ribs, this growth is less pronounced, and the maximum of acceleration of radiation transitions is displaced from the metal surface to the cavity axis. Besides, Purcell factor averaged in orientations of the dipole is hardly dependent on the angular position of the dipole inside the cavity, despite the fact that the cylindrical symmetry is disturbed due to the effect of the neighboring cavities of the periodical structure. The closeness of the maximum of Purcell factor depending on the wavelength of the emitting dipole to the maximum spectrum of chemiluminescence of luminol confirms the fitness of the aluminum film with the selected parameters of the cavities for the acceleration of chemiluminescence, and accordingly, increase of its intensity, since the latter depends on the competition between the radiation and non-radiation transitions. The ability of the considered nanostructure to reinforce the chemiluminescent radiation makes it promising for increase of the sensitivity of chemiluminescent biosensors.

Funding

This study was supported by the Russian Science Foundation, grant № 23-72-00045, <https://rscf.ru/project/23-72-00045/>.

Conflict of interest

The authors declare that they have no conflict of interest.

References

- [1] M.A. Tzani, D.K. Gioftsidou, M.G. Kallitsakis, N.V. Pliatsios, N.P. Kalogiouri, P.A. Angaridis, N.L. Ioan-

- nis, M.A. Terzidis. *Molecules*, **26** (24), 7664 (2021).
DOI: 10.3390/molecules26247664
- [2] A. Compagnone, A. Matheeußen, L. De Vooght, P. Cos. *Sci. Rep.*, **13** (1), 12203 (2023).
DOI: 10.1038/s41598-023-39397-8
- [3] Y. Cao, J. Yang, B. Liu, Z. Li. *Chemical & Biomedical Imaging*, **3** (12), (2025). DOI: 10.1021/cbmi.5c00043
- [4] M. Abdesselem, N. Pétri, R. Kuhner, F. Mousseau, V. Rouffiac, T. Gacoin, C. Laplace-Builhé, A. Alexandrou, C.I. Bouzigues. *Biomed. Opt. Express*, **14** (10), 5392 (2023).
DOI: 10.1364/BOE.501914
- [5] M.C. Cabello, F.H. Bartoloni, E.L. Bastos, W.J. Baader. *Biosensors (Basel)*, **13** (4) 452 (2023).
DOI: 10.3390/bios13040452
- [6] K. Aslan, C.D. Geddes. *Chem. Soc. Rev.*, **38** (9), 2556 (2009).
DOI: 10.1039/B807498B
- [7] D.R. Dadadzhanov, I.A. Gladskikh, M.A. Baranov, T.A. Vartanyan, A. Karabchevsky. *Sensors and Actuators B: Chemical*, **333**, 129453 (2021).
DOI: 10.1016/j.snb.2021.129453
- [8] D.R. Dadadzhanov, A.V. Palekhova, T.A. Vartanyan. *Opt. Spectrosc.*, **131** (12), 1646 (2023).
DOI: 10.61011/EOS.2023.12.58186.5850-23.
- [9] D.V. Kononov, A.V. Palekhova, N.A. Filatov, N.B. Leonov, A.S. Bukatin, D.R. Dadadzhanov, T.A. Vartanyan. *Opt. and spektr.*, (in Russian) **132** (12), 1300–1304 (2024).
- [10] A. Ramos-Velazquez, A. Belashov, A. Bondarenko, D. Sinev, P. Filatov, D. Kononov, A. Tiushkevich, T. Vartanyan, D. Dadadzhanov, G. Romanova. *Opt. and Quant. Electr.*, **57** (5), 277 (2025).
- [11] N.S. Petrov, D.R. Dadadzhanov, T.A. Vartanyan. *Opt. i spektr.*, **133** (1), 100–106 (2025) (in Russian).
DOI: 10.61011/OS.2025.01.59885.7341-24
- [12] K.M. McPeak, S.V. Jayanti, S.J.P. Kress, S. Meyer, S. Iotti, A. Rossinelli, D.J. Norris. *ACS Photonics*, **2** (3), 326 (2015).
DOI: 10.1021/ph5004237

Translated by M.Verenikina